



Articles All fields Author
 Images Journal/Book title Volume Issue Page

Connect with over 375,000 life-sciences researchers. [Register for free](#) **BiomedExpress**
 Your scientific professional network

[PDF \(137 K\)](#) [Export citation](#) [E-mail article](#)

Article [Figures/Tables \(6\)](#) [References \(20\)](#) [Thumbnails](#) | [Full-Size images](#)

Engineering Analysis with Boundary Elements
 Volume 22, Issue 3, October 1998, Pages 245-250

doi:10.1016/S0955-7997(98)00041-1 | [How to Cite or Link Using DOI](#)
[Permissions & Reprints](#)

Research Note

Two-dimensional time-harmonic dynamic coupled thermoelasticity analysis by boundary element method formulation

Parissa Hosseini Tehrani, Mohamad Reza Eslami

Mechanical Engineering Department, Amirkabir University of Technology (Tehran Polytechnic), Hafez Avenue No. 424, Tehran 15914, Iran

Received 1 December 1997; Accepted 1 April 1998. Available online 6 January 1999.

Abstract

A boundary element method is developed for time-harmonic analysis of a finite two-dimensional structure in dynamic coupled thermoelasticity. The advantage of the proposed technique is although it assumes a harmonic excitation, domain discretization is not required and a single region analysis can be done. The boundary integral equations of displacement and temperature fields are considered and a single thermal

Rela

- [A nev Engir](#)
- [Appli Engir](#)
- [Evalu Engir](#)
- [The s Journ](#)
- [A bo Engir](#)

[View](#)

My Ap

[Add](#)



Find down

[About](#)

excitation is used to derive the boundary element equilibrium equations. Comparison is made and the coupling effect in natural frequencies, resonance amplitudes and temperature distribution is investigated.



Keywords: Coupled thermoelasticity; Time-harmonic; Resonance frequencies; Boundary element

Article Outline

1. [Introduction](#)
2. [Governing equations](#)
3. [Boundary integral equation](#)
4. [Fundamental solution](#)
5. [Numerical examples](#)
6. [Conclusions](#)

References

1. Introduction

Thermodynamic laws predict the strain rate variations in a solid body to be accompanied by temperature variations which, in turn, cause heat flows. The latter gives rise to entropy and, consequently, to dissipation of vibrational energy. The process, commonly referred to as “thermoelastic damping”, is contained in the coupled system of differential equations that describes the deformation and heat flow in a continuum. When a material body is subjected to an external disturbance it transmits mechanical waves. For example, sudden heat deposition in a solid body will create a mechanical wave through thermal expansion.

If the heat deposition occurrence is within a short time span, it creates thermal stress waves and consequently the coupled equations of thermoelasticity and energy must be considered simultaneously. The classical coupled equations can be described either in time or frequency domains. Although there are many papers dealing with coupled thermoelasticity problems in time domain, seldom is the problem discussed in the frequency domain.

The study of the time-harmonic problem is one of the most extensive and productive areas of continuum dynamics. Time-harmonic problems are those in which all the time-dependent variables vary with time as $\sin \omega t$ or $\cos \omega t$, ω being the angular frequency. Using complex notation, the time dependence is written as $\exp i\omega t$ or $\exp -i\omega t$.

There are several reasons why the study of time-harmonic problems is important and productive. First, the solution to the governing equations are very much simplified in this case. The Navier equations are simplified to equations containing only space derivatives. The convolution products in the reciprocal theorem and integral representation become simple dot products for this case. The simplification of the equations allows for the analytical solution of some basic problems which cannot be solved for other time dependencies. A second reason for the importance of harmonic problems is that elastic regions, and in general regions governed by the wave equation, under homogeneous boundary conditions, oscillate harmonically with natural frequencies of the system which are an infinite sequence. Finally, a third reason is based on the fact that harmonic functions constitute a complete class of independent functions. Information concerning classical dynamic thermoelasticity can be found in the work of Biot [1], Chadwick [2], and Nowacki [3].

The dynamic propagation of plane waves in coupled thermoelastic solids has been studied by several authors. Nayfeh and Nemat-Nasser [4] studied the effects of the thermal coupling on both plane harmonic

Cite

- [Trans Struc](#)
- [Boun Jourr](#)
- [Boun Jourr](#)
- [View](#)

Relat

- [BOUI Ency](#)
- [2.37 · Shrei](#)
- [STR1 FREC Ency](#)
- [Prefa Comj](#)
- [3.02 · Comj](#)
- [More](#)

[View F](#)

Jobs

[Post](#)

[See](#)

[Sign](#)

[See](#)

- [Ass Phil Mar](#)

thermoelastic waves in unbounded media, and Rayleigh's surface waves propagation along the free surface of a half-space. Later, Puri [5], obtained exact solutions to the frequency equation, and calculated exact values for the real and imaginary parts of the wave number. Agarwal [6] determined phase velocity, attenuation coefficient, and amplitude ratio behavior for quasi-elastic and quasi-thermal modes by directly solving the frequency equation. All of the above-mentioned studies are in an infinite domain.

Time-domain boundary element method (BEM) to quasi-static thermoelastic problems were first provided by Dargush and Banerjee [7] and [8]. In the realm of classical dynamic thermoelasticity, the well-known fundamental solution in the transform domain by Nowaki [9] and the reciprocal theorem by Ionescu-Cazimir [10] have been available for a long time. On the other hand, several authors [11] have written various forms of fundamental solution and integral representation for the classical theory, but no BEM application has been reported to verify the validity of these formulations. Furthermore, nothing has appeared concerning time-harmonic coupled thermoelasticity in a finite domain.

It is possible to establish an analogy between poroelasticity and thermoelasticity design for a time-harmonic regime, as pointed out by Bonnet and Boutin [12]. They have shown that only solid displacements and fluid pressure or temperature are independent variables for poroelastic or thermoelastic problems. More recently, Cheng and Badmus [13] and Dominguez [14] developed frequency domain BEMs for dynamic poroelasticity in terms of independent variables. Both papers contain numerical implementations and applications, which are limited in scope to two-dimensional time-harmonic problems. Wagner [15] presented the fundamental matrix of the system of coupled thermoelasticity in one-dimension and obtained some results about coupling effects on temperature and displacement distribution.

In this paper, the boundary element formulation for time-harmonic dynamic coupled thermoelasticity problems in a two-dimensional finite domain is presented. A single heat excitation is used to drive the boundary element formulations. The influence of coupling parameter in natural frequencies, temperature and displacement distribution is discussed. Amplitude versus frequency in resonance condition for various coupling parameters is investigated and new information is derived from the so-called chart and graphs. Throughout this paper, the summation convention on repeated indices is used. A dot indicate time differentiation and the subscript i after a comma is partial differentiation with respect to x_i ($i=1,2$).

2. Governing equations

A homogeneous isotropic thermoelastic solid is considered. In the absence of body forces and heat flux, the governing equations for the dynamic coupled thermoelasticity in the time domain can be written, in accordance with Kupradze et al. [16], as follows:

$$(\lambda + \mu) u_{j,jj} + \mu u_{i,jj} - \rho \ddot{u}_i - \gamma T_{,i} = 0 \quad (1)$$

$$kT_{,ii} - \rho c_e \dot{T} - \gamma T_0 u_{j,j} = 0 \quad (2)$$

where λ , μ , u_i , ρ , T , T_0 , k , γ and c_e are Lamé's constant, the components of displacement vector, density, absolute temperature, reference temperature, conductivity, stress-temperature modulus and specific heat respectively. It is convenient to introduce the usual dimensionless variables as follows:

$$\hat{x} = \frac{x}{\alpha}; \quad \hat{t} = \frac{t C_1}{\alpha}; \quad \hat{\sigma}_{ij} = \frac{\sigma_{ij}}{\gamma T_0}; \quad \hat{u}_i = \frac{(\lambda + 2\mu) u_i}{\alpha \gamma T_0}; \quad \hat{T} = \frac{T - T_0}{T_0} \quad (3)$$

where $a=k/\rho c_e C_1$ is the dimensionless unit length and $C_1 = \sqrt{(\lambda + 2\mu) / \rho}$ is the velocity of the longitudinal wave.

(1) and (2) take the form (dropping the hat for convenience):

$$\frac{\mu}{\lambda + 2\mu} u_{i,jj} + \frac{\lambda + \mu}{\lambda + 2\mu} u_{j,ij} - T_{,i} - \bar{u}_i = 0 \tag{4}$$

$$T_{,ii} - \bar{T} - \frac{T_0 \gamma^2}{\rho c_e (\lambda + 2\mu)} \dot{u}_{j,j} = 0 \tag{5}$$

Transferring (4) and (5) to frequency domain yields

$$\frac{\mu}{\lambda + 2\mu} u_{i,jj} + \frac{\lambda + \mu}{\lambda + 2\mu} u_{j,ij} - T_{,i} + \omega^2 u_i = 0 \tag{6}$$

$$T_{,ii} - i\omega T - \frac{T_0 \gamma^2}{\rho c_e (\lambda + 2\mu)} i\omega u_{j,j} = 0 \tag{7}$$

(6) and (7) are rewritten in matrix form as

$$L_{ij} U_j = 0 \tag{8}$$

For a two-dimensional domain the operator L_{ij} reduces to

$$L_{ij} = \begin{bmatrix} \frac{\mu}{\lambda + 2\mu} \Delta + \frac{\lambda + \mu}{\lambda + 2\mu} D_1^2 + \omega^2 & \frac{\lambda + \mu}{\lambda + 2\mu} D_1 D_2 & - D_1 \\ \frac{\lambda + \mu}{\lambda + 2\mu} D_1 D_2 & \frac{\mu}{\lambda + 2\mu} \Delta + \frac{\lambda + \mu}{\lambda + 2\mu} D_2^2 + \omega^2 & - D_2 \\ - \frac{T_0 \gamma^2}{\rho c_e (\lambda + 2\mu)} i\omega D_1 & - \frac{T_0 \gamma^2}{\rho c_e (\lambda + 2\mu)} i\omega D_1 & \Delta - i\omega \end{bmatrix}$$

$$U_i = [U \quad V \quad T]$$

where $D_i = \partial/\partial x_i$ ($i=1,2$) and Δ denotes the Laplacian. The boundary conditions are assumed to be as follows:

$$\begin{aligned} u_i &= \bar{u}_i & \text{on } \Gamma_u \\ \tau &= \sigma_{ij} n_j & \text{on } \Gamma_\tau \\ T &= \bar{T} & \text{on } \Gamma_T \\ q &= q_i n_i & \text{on } \Gamma_q \end{aligned} \tag{9}$$

where

$$\sigma_{ij} = \left(\frac{\lambda}{\lambda + 2\mu} u_{k,k} - T \right) \delta_{ij} + \frac{\mu}{\lambda + 2\mu} (u_{ij} + u_{ji}) \tag{10}$$

3. Boundary integral equation

In order to drive the boundary integral problem, we start with the following weak formulation of the differential equation set in Eq. (8) for the fundamental solution tensor V_{ik}^* :

$$\int_{\Omega} (L_{ij} U_j) V_{ik}^* d\Omega = 0 \tag{11}$$

After integrating by parts over the domain and taking a limiting procedure approaching the internal source point to the boundary point, we can obtain the following boundary integral equation:

$$C_{kj} U_k(y, \omega) = \int_{\Gamma} \tau_{\alpha}(x, \omega) V_{\alpha j}^*(x, y, \omega) - U_{\alpha}(x, \omega) \Sigma_{\alpha j}^*(x, y, \omega) d\Gamma(x) + \int_{\Gamma} T_{,n}(\tag{12}$$

where $U_{\alpha}=u_{\alpha}$ ($\alpha=1,2$) and $U_3=T$ and C_{kj} denotes the shape coefficient tensor. The kernel $\Sigma_{\alpha j}^*$ in Eq. (12) is defined by

$$\Sigma_{\alpha j}^* = \left[\left(\frac{\lambda}{\lambda + 2\mu} V_{ik,k}^* + \frac{T_0 \gamma^2}{\rho C_e (\lambda + 2\mu)} i\omega V_{3j}^* \right) \delta_{\alpha\beta} + \frac{\mu}{\lambda + 2\mu} (V_{\alpha j,\beta}^* + V_{\beta j,\alpha}^*) \right] n_{\beta} \tag{13}$$

Here the fundamental solution tensor V_{jk} must be determined as the tensor which satisfies the differential equation

$$l_{ij} V_{jk}^* = -\delta_{ik} \delta(x - y) \tag{14}$$

Where l_{ij} is the adjoint operator of L_{ij} in Eq. (8) and given by

$$l_{ij} = \begin{bmatrix} \frac{\mu}{\lambda + 2\mu} \Delta + \frac{\lambda + \mu}{\lambda + 2\mu} D_1^2 + \omega^2 & \frac{\lambda + \mu}{\lambda + 2\mu} D_1 D_2 & -\frac{T_0 \gamma}{\rho C_e (\lambda + 2\mu)} \\ \frac{\lambda + \mu}{\lambda + 2\mu} D_1 D_2 & \frac{\mu}{\lambda + 2\mu} \Delta + \frac{\lambda + \mu}{\lambda + 2\mu} D_2^2 + \omega^2 & -\frac{T_0 \gamma}{\rho C_e (\lambda + 2\mu)} \\ -D_1 & -D_2 & \Delta - i\omega \end{bmatrix}$$

4. Fundamental solution

In order to construct the fundamental solution we put the fundamental solution tensor V_{ij}^* of Eq. (14) in the following potential representation by using the transposed co-factor operator μ_{ij} of l_{ij} and scalar function Φ^* [17]:

$$V_{ij}^*(x, y, \omega) = \mu_{ij} \Phi^*(x, y, \omega) \tag{15}$$

After substitution of Eq. (15) into Eq. (14), we can get the following differential equations:

$$A \Phi^* = -\delta(x - y) \tag{16}$$

where

$$A = \det(l_{ij}) = \frac{\mu}{\lambda + 2\mu} (\Delta + h_1^2)(\Delta + h_2^2)(\Delta + h_3^2) \tag{17}$$

and h^2_i are solutions of

$$h^2_1 = \frac{\lambda + 2\mu}{\mu} \omega^2 \tag{18}$$

$$h^2_2 + h^2_3 = \omega^2 - i\omega \left[1 + \frac{T_0 \gamma^2}{\rho c_e (\lambda + 2\mu)} \right] h^2_2 h^2_3 = -i\omega^3$$

where h_1 is the longitudinal wave velocity, h_2 is the thermal wave velocity, and h_3 is the rotational wave velocity and

$$\Phi = \frac{\lambda + 2\mu}{2\pi\mu} \left[\frac{K_0(i h_1 r)}{(h^2_2 - h^2_1)(h^2_3 - h^2_1)} + \frac{K_0(i h_2 r)}{(h^2_3 - h^2_2)(h^2_1 - h^2_2)} + \frac{K_0(i h_3 r)}{(h^2_1 - h^2_3)(h^2_2 - h^2_3)} \right] \tag{19}$$

The fundamental solution tensor V^*_{ij} for the two-dimensional domain is found as follows:

$$V^*_{\alpha\beta} = \sum_{k=1}^3 (\psi_k(r) \delta_{\alpha\beta} + \kappa_k r_{,\alpha} r_{,\beta}) \quad (\alpha, \beta = 1, 2) \tag{20}$$

$$V^*_{3\alpha} = \sum_{k=1}^3 \xi_k(r) r_{,\alpha}$$

$$V^*_{\alpha 3} = \sum_{k=1}^3 \xi_k(r) r_{,\alpha}$$

$$V^*_{33} = \sum_{k=1}^3 \zeta_k(r)$$

where

$$\psi_k(r) = \frac{W_k}{2\pi} \left\{ (-h^2_k + m_2)(-h^2_k - m_1) + \left(\frac{\lambda + \mu}{\mu} \right) \left[h^2_k + m_1 \left(1 + C \frac{\lambda + 2\mu}{\lambda + \mu} \right) \right. \right. \tag{21}$$

$$\left. \left. + \frac{W_k(\lambda + \mu)}{2\pi\mu} \left[-h^2_k - m_1 \left(1 + C \frac{\lambda + 2\mu}{\lambda + \mu} \right) \right] \frac{i h_k}{r} K_1(i h_k r) \kappa_k(r) = \frac{W_k(\lambda + \mu)}{2\pi\mu} \right. \right.$$

$$\left. = \frac{W_k}{2\pi} \left(-h^2_k + \frac{\lambda + 2\mu}{\mu} \omega^2 \right) i h_k K_1(i h_k r) \xi_k(r) = \frac{W_k}{2\pi} \delta i \omega \left(-h^2_k + \frac{\lambda + 2\mu}{\mu} \omega^2 \right) \right.$$

$$\left. = \frac{W_k}{2\pi} \left(-h^2_k + \frac{\lambda + 2\mu}{\mu} \omega^2 \right) (-h^2_k + \omega^2) K_0(i h_k r) \right.$$

and

$$r = \|x - y\| \quad m_1 = i\omega \quad m_2 = \frac{\lambda + 2\mu}{\mu} \omega^2 \quad C = \frac{T_0 \gamma^2}{\rho c_e (\lambda + 2\mu)} \quad W_i = \frac{-1}{(h^2_i - h^2_j)(h^2_k)} \tag{22}$$

5. Numerical examples

The two-dimensional vibration of square cantilever plate has been studied by Gupta [18]. He considered the plane stress condition, and with a very fine finite element mesh obtained a very accurate solution. This “accurate solution” has been used by Cook and Avrashi [19] and Zhao and Steven [20] to assess the accuracy of different alternative solutions for the same problem. For this reason, it seems reasonable that

the in-plane vibration of a square cantilever plate under the plane stress condition should serve as a standard problem, against which any new solution technique can be examined.

As shown in Fig. 1, a square cantilever plate subjected to an oscillation temperature $T = T_0 e^{i\omega t}$ at a fixed edge is considered. The length and width are equal to 2 (non-dimensional), Poisson's ratio is equal to 0.3 and the plate is thermally isolated at three other edges.

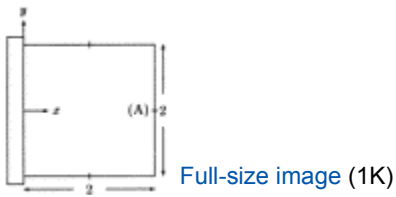


Fig. 1.

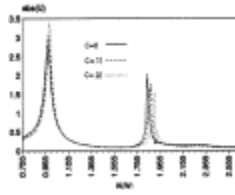
BEM model of a square cantilever plate.

Table 1 shows a comparison between the exact solution and the BEM solution with different coupling parameters for the natural frequency of the vibration of the square cantilever plate at point (A).

Table 1. Comparison between exact natural frequency normalized by first natural frequency of free vibration and numerical BEM solutions with different coupling parameter

$\bar{\omega} = W / W_1$	Exact solution	C=0	C=0.45	C=1
$\bar{\omega}_1$	1.	0.975	0.983	0.989
$\bar{\omega}_2$	1.770	1.845	1.885	1.905
$\bar{\omega}_3$	2.032	1.927	1.930	1.934

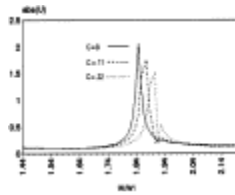
Fig. 2 shows the distribution of the absolute vibration's amplitudes along the X-direction at point (A) versus the normalized frequency ratio, W/W_1 being the first natural frequency of free vibration. In this figure the effect of the coupling parameter on the resonance frequencies and amplitudes is shown. The first three resonance frequencies are detected in the figure. The first one is around $W/W_1=0.975$, the second is around $W/W_1=1.845$, and the third one is around $W/W_1=1.927$. However, the third resonance is not very clear from Fig. 2; Fig. 3 is the scale-up around the second and third natural frequencies. Since the excitement of higher modes requires larger input energy, the third mode amplitude for this problem is small. Table 1, Fig. 2 and Fig. 3 show that the coupling term has a different effect on different modes. It seems that the coupling term has a similar effect on the first and third modes, whereas it differs for the second mode. At the first and third modes, where \ddot{w}_i, \dot{w}_i is positive at point (A), the increase of the coupling parameter causes a decrease of temperature distribution. The decreased temperature causes smaller thermal damping in the system and the natural frequencies approach the case of free vibration, while the related amplitudes increase. At the second natural frequency, where \ddot{w}_i, \dot{w}_i is negative at point (A), the increase of the coupling parameter causes an increase of temperature distribution. Consequently, the system becomes more resistant to compression and deviates from the case of the free vibration. The vibration amplitude in this case decreases.



[Full-size image \(6K\)](#)

Fig. 2.

Coupling effect on resonance frequencies and amplitude.

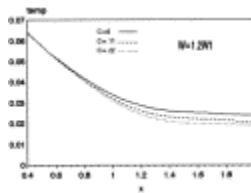


[Full-size image \(5K\)](#)

Fig. 3.

Coupling effect on resonance amplitude in second and third natural frequencies.

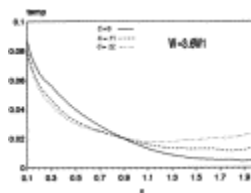
Fig. 4 Fig. 5 show the temperature distribution along the axis of symmetry (X -axis) for different coupling parameters for specified W/W_1 . Around the first mode, where $W/W_1=1.2$, Fig. 4 shows that the increase of the coupling parameter has a decreasing effect on the temperature distribution. At higher modes, as shown in Fig. 5 for $W/W_1=3.6$, the coupling effect may have different effects on the temperature distribution, depending upon the mode shapes.



[Full-size image \(5K\)](#)

Fig. 4.

Coupling effect on temperature distribution along the axes of symmetry of a plate.



[Full-size image \(5K\)](#)
















Fig. 5.






Coupling effect on temperature distribution along the axes of symmetry of a plate.

6. Conclusions

A BEM is developed for time-harmonic analysis of a finite two-dimensional structure in dynamic coupled thermoelasticity. The advantage of the proposed technique assumes a harmonic excitation, domain discretization is not required and a single region analysis can be done. The boundary integral equations of displacement and temperature fields are considered and a single thermal excitation is used to derive the boundary element equilibrium equations. A comparison is made and the coupling effect in the natural frequencies, resonance amplitudes and temperature distribution is investigated.

References

- 1 M.A. Biot, Thermoelasticity and irreversible thermodynamics. *J. Appl. Phys.*, **27** (1956), pp. 240–253. 
- 2 Chadwick P. Thermoelasticity. The dynamical theory. In: Sneddon IN, Hill R, editors. Progress in solid mechanics, vol. 1. Amsterdam: North Holland, 1960:265–328.. 
- 3 Nowacki W. Dynamic problems of thermoelasticity. Leyden: Noordhoff, 1975.. 
- 4 A.H. Nayfeh and S. Nemat-Nasser, Thermoelastic waves in solid with thermal relaxation. *Acta Mech.*, **12** (1971), pp. 53–69. 
- 5 P. Puri, Plane waves in generalized thermoelasticity. *Int. J. Eng. Sci.*, **11** (1973), pp. 735–744. 
- 6 V.K. Agarwal, On plane waves in generalized thermoelasticity. *Acta Mech.*, **31** (1979), pp. 185–198. 
- 7 G.F. Dargush and P.K. Banerjee, Development of a boundary element method for time dependent planar thermoelasticity. *Int. J. Solid Struct.*, **25** (1989), pp. 999–1021. 
- 8 G.F. Dargush and P.K. Banerjee, Boundary element methods in three-dimensional thermoelasticity. *Int. J. Solid Struct.*, **26** (1990), pp. 199–216. 
- 9 W. Nowacki, Green functions for the thermoelastic medium. *I. Bull. Acad. Polon. Ser. Techn.*, **12** (1964), pp. 315–321. 
- 10 V. Ionescu-Cazimir, Problem of linear thermoelasticity. Theorems on reciprocity for dynamic problem of thermoelasticity. *I. Bull. Acad. Polon. Ser. Techn.*, **12** (1964), pp. 473–488. 
- 11 V. Sladek and J. Sladek, Boundary integral equation method in thermoelasticity. Part I: general analysis. *Appl. Math. Modelling*, **7** (1984), pp. 241–253. 
- 12 C. Boutin and G. Bonnet, Green functions and associated sources in infinite and stratified poroelastic media. *Geophys. J. R. Astr. Soc.*, **90** (1987), pp. 521–550. 
- 13 A.H.D. Cheng and T. Badmus, Integral equation for dynamic poroelasticity in frequency domain with BEM solution. *ASCE J. Engng. Mech.*, **117** (1991), pp. 1136–1158. 
- 14 J. Dominguez, Boundary element approach for dynamic poroelastic problem. *Int. J. Num. Meth. Engng.*, **35** (1992), pp. 307–324. 
- 15 P. Wagner, Fundamental matrix of the system of dynamic linear thermoelasticity. *J. Thermal Stresses*, **17** (1994), pp. 549–569. 

- 16 Kupradze VD, Gegelia IG, Basheleishvili MO, Burchuladze IV. Three-dimensional problems of the mathematical theory of elasticity and thermoelasticity. Amsterdam: North-Holland, 1985.. 
- 17 Tosaka N. Boundary integral equation formulations for linear coupled thermoelasticity. Proc. 3rd. Japan Symp. on BEM Jascome, Tokyo, 1986:207–212.. 
- 18 K.K. Gupta, Development of a finite dynamic element for free vibration analysis of two-dimensional structure. *Int. J. Num. Meth. Engng.*, **12** (1978), pp. 1311–1327. 
- 19 R.D. Cook and J. Avrashi, Error estimation and adaptive meshing for vibration problems. *Comput. Struct.*, **44** (1992), pp. 619–626. 
- 20 C. Zhao and P. Steven, Asymptotic solutions for predicted natural frequencies of two-dimensional elastic solid vibration problems in finite element analysis. *Int. J. Num. Meth. Engng.*, **39** (1996), pp. 2821–2835. 



Corresponding author

Copyright © 1998 Elsevier Science Ltd. All rights reserved.

Engineering Analysis with Boundary Elements
Volume 22, Issue 3, October 1998, Pages 245-250

[Home](#) [Browse](#) [Search](#) [My settings](#) [My alerts](#) [Shopping cart](#)

About ScienceDirect
[What is ScienceDirect](#)
[Content details](#)
[Set up](#)
[How to use](#)
[Subscriptions](#)
[Developers](#)

Contact and Support
[Contact and Support](#)

About Elsevier
[About Elsevier](#)
[About SciVerse](#)
[About SciVal](#)
[Terms and Conditions](#)
[Privacy policy](#)
[Information for advertisers](#)

Copyright © 2011 [Elsevier B.V.](#) All rights reserved. SciVerse® is a registered trademark of Elsevier Properties S.A., used under license Elsevier B.V.